Negative Photoresponses in MoS_2 Flakes Photogated by p-n Junction Diode

Yumeng Liu, Jianyong Wei, Seyed Saleh Mousavi Khaleghi, Yizhuo Wang, Zhengfang Fan, Shuwen Guo, Wenhan Song, Zhentao Lian, Zhijuan Su, Hao Wei, Robert Kudrawiec, Rui Yang, *Member, IEEE*, and Yaping Dan, *Senior Member, IEEE*

***Abstract*— Negative photoresponses in photodetectors can find important applications like image AI and image edge detection. In this Letter, we develop a few-layer MoS_2 phototransistor photogated by a silicon-based N^+P junction. Negative photovoltage will be generated on the open-circuit N^+P junction by grounding the p-type substrate. The negative photovoltage modulates the conductance of the n-type MoS_2 flake, creating negative photoconductance in the MoS_2 channel. The light-intensity dependent photoresponses are characterized at cryogenic temperatures. The experimental results can be well fitted with the established device theory.**

***Index Terms*— MoS_2, photoresponse, PN junction.**

I. Introduction

NEGATIVE photoresponses in photodetectors can find important applications in image AI [1], [2], image edge detection [3], [4], optoelectronic memory [5], optoelectronic detection [6] and low power consume device [7]. The light-induced current suppression enables on-chip differential signal processing, offering inherent contrast enhancement and edge detection capabilities that are unattainable with conventional single-polarity photodetectors. Negative photoresponses have been reported in photodetectors made of either nanowires [8], [9], heterogeneous semiconductor structures [10], [11], 2D materials [12], [13], [14], [15] or graphene [16], [17]. Most of these negative photoresponses arise from the trapping effect of defect states [18], [19] which are disadvantageous in the following two aspects. First, the trapping and emission lifetime of defect states are often at a scale of seconds or even longer. The resultant negative photoresponses are too slow to find practical applications. Second, defect states are difficult to engineer. By contrast, techniques to suppress the defect states have been well developed in commercial semiconductor technologies [20]. As a result, there is little opportunity for these negative photoresponse devices that rely on defect states to find practical applications.

In this Letter, we present a novel approach to realizing negative photoconductivity in MoS_2 phototransistors by integrating a silicon-based NP junction in the substrate as an external photogate. Upon light illumination, the NP junction generates a negative open-circuit photovoltage, which electrostatically modulates the MoS_2 channel conductance, leading to robust and controllable negative photoresponses without relying on defect states. This mechanism enhances device stability and tunability, offering new possibilities for advanced optoelectronic applications. Light-intensity-dependent photoresponses at cryogenic temperatures are also systematically investigated.

II. Results And Discussion

Fig. 1(a) illustrates the schematic design of our device structure, comprising a silicon-based PN junction diode with a few layers of MoS_2 deposited on the top. A 5 nm thick hafnium oxide (HfO_2) layer serves as the gate dielectric on the PN junction. Upon illumination, the PN junction diode generates a an open-circuit voltage, which electrically gates the MoS_2 transistor. Fig. 1(b) shows the optical microscopic image of such a typical device in the top view, where the gray area marked with red dashed line denotes the highly doped region of the PN junction, while the blue line indicates the MoS_2 flake.

Received 18 April 2025; accepted 30 April 2025. Date of publication 9 May 2025; date of current version 1 July 2025. This work was supported in part by the Oceanic Interdisciplinary Program of Shanghai Jiao Tong University under Grant SL2022ZD107; in part by the National Key Laboratory of Infrared Detection Technologies under Grant IRDT-23-10; in part by the National Science Foundation of China (NSFC) under Grant 62304131, Grant 92364107, and Grant W2412118; and in part by the Science and Technology Commission of Shanghai Municipality (STCSM) under Grant 23QA1405300 and Grant 24ZR1491500. The review of this letter was arranged by Editor S. Zhang. *(Corresponding authors: Zhijuan Su; Yaping Dan.)*

Yumeng Liu and Zhengfang Fan are with the University of Michigan–Shanghai Jiao Tong University Joint Institute, Shanghai 200240, China, and also with the Department of Micro/Nano Electronics, School of Electronic Information and Electrical Engineering, Shanghai Jiao Tong University, Shanghai 200240, China.

Jianyong Wei, Yizhuo Wang, Wenhan Song, Zhentao Lian, and Rui Yang are with the University of Michigan–Shanghai Jiao Tong University Joint Institute, Shanghai 200240, China.

Seyed Saleh Mousavi Khaleghi is with the University of Michigan–Shanghai Jiao Tong University Joint Institute, Shanghai 200240, China, and also with the Department of Electrical and Electronic Engineering, The University of Melbourne, Parkville, VIC 3010, Australia.

Shuwen Guo is with the School of Energy and Materials, Shanghai Polytechnic University, Shanghai 201209, China.

Zhijuan Su is with the State Key Laboratory of Micro-Nano Engineering Science and the Global Institute of Future Technology, Shanghai Jiao Tong University, Shanghai 200240, China (e-mail: zhijuan.su@sjtu.edu.cn).

Hao Wei is with the Department of Micro/Nano Electronics, School of Electronic Information and Electrical Engineering, Shanghai Jiao Tong University, Shanghai 200240, China.

Robert Kudrawiec is with the Department of Semiconductor Materials Engineering, Wrocław University of Science and Technology, 50-370 Wrocław, Poland.

Yaping Dan is with the University of Michigan–Shanghai Jiao Tong University Joint Institute, Shanghai 200240, China, and also with the State Key Laboratory of Micro-Nano Engineering Science, Shanghai Jiao Tong University, Shanghai 200240, China (e-mail: yaping.dan@sjtu.edu.cn).

Digital Object Identifier 10.1109/LED.2025.3568545

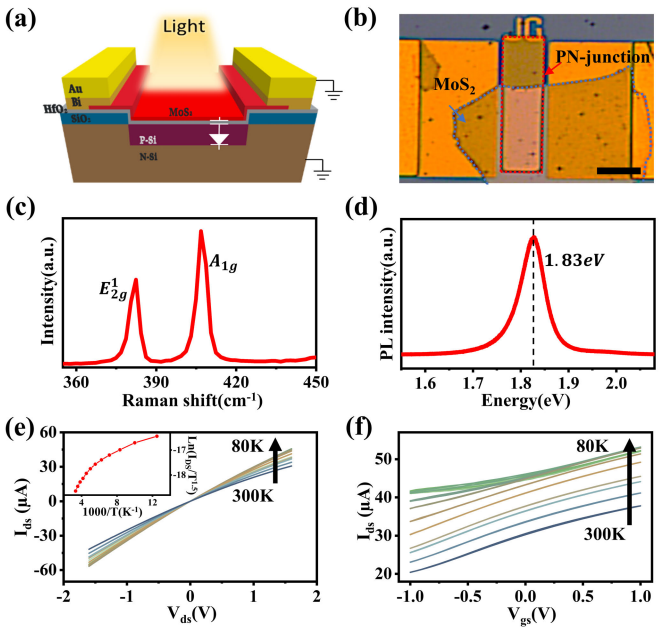

Fig. 1. (a) 3D Schematic of the device with a PN junction. (b) Optical microscopy image of a fabricated device. The reference bar is 50μm. (c) Raman spectroscopy of MoS_2 and (d) Photoluminescence spectrum of MoS_2 under green laser excitation ($\lambda = 532$ nm). (e) The output characteristic of the device varies at different temperatures with the grounded substrate. Inset: Arrhenius plot of the absolute dark current at a fixed drain-source voltage of -1.6 V. (f) Gate dependent source-drain current at different cryogenic temperature.

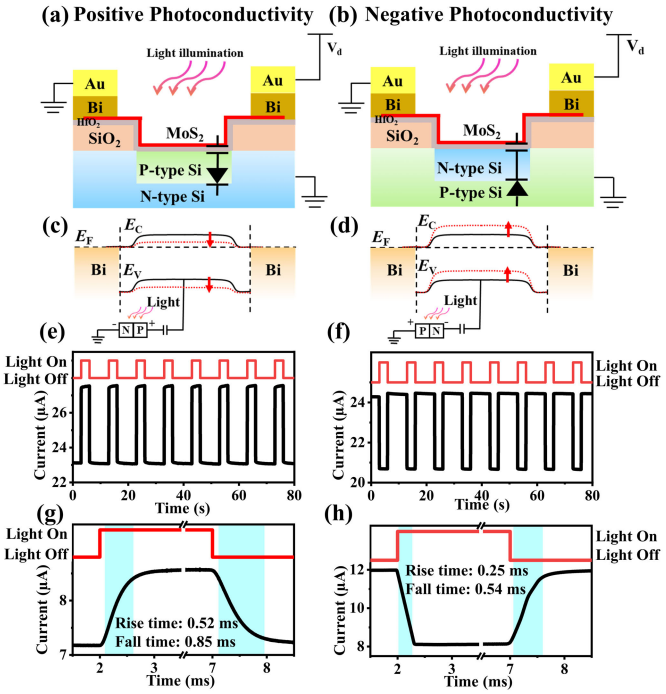

Fig. 2. Schematic of the device with a PN junction (a) and the one with a NP junction (b). Band diagram of the device from equilibrium conditions to under light illumination with a PN junction (c) and with a NP junction (d). Current transients (normalized by the channel width-to-length ratio) of the (e) positive and (f) negative photoresponse device at a bias of 1 V, where illumination at $\lambda = 780$ nm is pulsed ON/OFF periodically. Transient response of the photodetector with a PN junction (g) and with an NP junction (h) at 780nm. The rise time and fall time is calculated based on 10% and 90% levels of device current.

The device fabrication process is described in the following. For P^+N junctions, a p-type region (10^{19}cm^{-3}) is created by ion implantation of boron on an n-type silicon substrate with a phosphorus doping concentration of 1-5 $\times 10^{15}$cm^{-3}. For N^+P junctions, an n-type region (10^{20}cm^{-3}) is created by ion implantation of phosphorus on a p-type silicon substrate with a boron doping concentration of 2-8 $\times 10^{15}$cm^{-3}. Subsequently, 5nm thick HfO_2 is deposited on the junction via atomic layer deposition. A few-layer MoS_2 flake is then transferred onto the junction using a gold-assisted transfer technique [21], followed by the thermal evaporation of a 100 nm/20nm thick Au/Bi electrode to form electrical contacts with the MoS_2 layer.

To evaluate the material quality of the MoS_2 flakes, Raman and photoluminescence (PL) spectroscopy were conducted on the sample. The Raman spectrum in Fig. 1(c) shows two distinct peaks associated with the E^1_{2g} and A_{1g} vibrational modes of MoS_2. The separation between these peaks is measured at 24.19 cm^{-1}, indicating that the sample is a few-layer MoS_2 flake [22]. The PL spectrum, acquired with green laser excitation ($\lambda = 532$ nm), is displayed in Fig. 1(d), showing a prominent peak at 1.83 eV, consistent with the fact that the MoS_2 flake has a bandgap of 1.8eV [23], [24].

Fig. 1(e) presents the current-voltage (IV) characteristics at different temperatures. Due to the fact that the substrate is grounded, the IV curves are slightly nonlinear at positive drain bias, similar to the channel pinch-off phenomenon in the classical metal-oxide-semiconductor field effect transistor (MOSFET). To investigate how the conductance is dependent on temperature, we plot the current at a fixed negative drain bias (-1.6V) at different temperature in the Arrhenius plot shown in the inset of Fig. 1(e). The positive slope observed in the Arrhenius plot confirms the Ohmic contacts between the bismuth electrodes and the few-layer MoS_2 channel [25], [26]. The gate dependent current indicates that the MoS_2 channel is n-type as shown in Fig. 1(f).

Previously, we have systematically investigated the MoS_2 device photogated by a PN junction in the substrate [27]. Such a device shows positive photoresponses. Interestingly, negative photoresponses are expected when the device is photogated by a NP junction in the substrate. Negative photoresponses can find important applications in image AI [1], [2] and image edge detection [3], [4]. Figure 2 presents a side-by-side comparison of the device for positive and negative photoconductivity, with their respective schematics shown in Fig. 2(a) and (b). The devices are illuminated by a 780 nm red LED (30% duty cycle), a wavelength deliberately chosen to exceed the absorption edge of MoS_2 ($\lambda = 680$ nm), ensuring that light is absorbed primarily by the silicon junction rather than the MoS_2 channel.

In the positive photoconductivity device (Fig. 2(a)), light absorption generates electron-hole pairs, inducing a positive open-circuit photovoltage that gates the MoS_2 channel and enhances its conductance (Fig. 2(c)). Conversely, in the negative photoconductivity device (Fig. 2(b)), the photogenerated carriers produce a negative photovoltage,

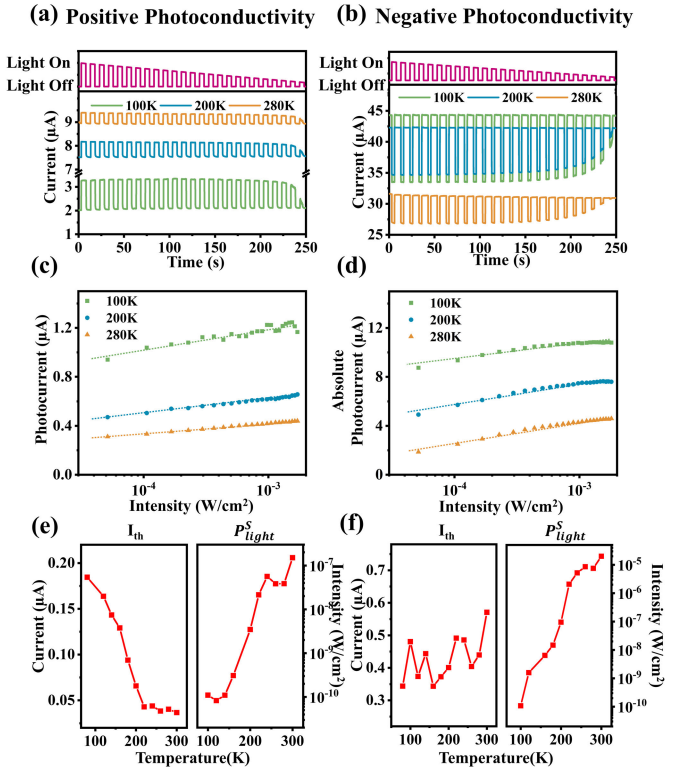

Fig. 3. (a) Positive and (b) negative photoconductivity device photocurrent at a fixed bias of 1V as illumination intensity decreases. The light wavelength is λ =780 nm and the temperature is lowered from 300 to 80K. Measured photocurrent vs illumination intensity for (c) positive and (d) negative photoresponse device. The parameters extracted from (c) positive and (d) negative photoresponses are presented in (e) and (f) as a function of temperature, respectively.

which depletes electrons in the n-type MoS_2 channel, leading to a reduction in current (Fig. 2(d)).

The opposing photoresponses are further confirmed by transient measurements (Fig. 2(e) (f)), where the PN device exhibits a current increase under illumination, while the NP device shows a clear current suppression. Both configurations achieve sub-millisecond response times (Fig. 2(g) (h)), demonstrating their potential for high-speed, polarity-tunable photodetection.

To investigate how the photoresponses are dependent on the illumination light intensity, we tune the light intensity linearly in each on/off cycle while monitoring the transient response in current. The photocurrent is logarithmically dependent on the light intensity as shown in Fig. 3(c) and (d), which can be well fitted with eq. (1) established in our previous work [27].

$$I_{ph} = I_{th}\ln\left(\frac{P_{light}}{P^s_{light}} + 1\right), \tag{1}$$

where P^s_{light} is the critical light intensity, indicating the detection limit of the device. The threshold current I_{th} is a parameter showing the response in current of the MoS_2 flake to the photogate voltage. The detailed expression of these parameters can be found in our previous publication [27]. From the fittings in Fig. 3(c) and (d), we can extract P^s_{light} and I_{th}.

The above experiments and fittings are repeated at different temperature. The extracted I_{th} and P^s_{light} for both positive and negative photoconductive devices are presented in Fig. 3(e) and (f) at different temperature, respectively. The observed changes in I_{th} are notably complicated, arising from the interplay of various factors, including charge trapping at interfaces, the minority carrier recombination lifetime [28], and the intrinsic and free electron concentrations [29]. In contrast, P^s_{light} exhibits a clear trend of decline as the temperature decreases. This behavior can be attributed to the reduction in the intrinsic carrier concentration n_i of the semiconductor at lower temperatures because of $P^s_{light} \sim n_i/\tau_0$ with τ_0 being the minority carrier recombination lifetime. The observed temperature dependence of P^s_{light} confirms that the device demonstrates an enhanced sensitivity to lower light intensities at low temperature, consistent with the semiconductor device principle. The difference of P^s_{light} in PN junction (10^{-10} – 10^{-7} W/cm^2) and NP junction (10^{-10} – 10^{-5} W/cm^2) arises from the fact that the doping concentrations in the latter case are higher, leading to a stronger temperature dependence of minority recombination lifetime τ_0 [28].

III. Conclusion

We demonstrate a MoS_2 phototransistor gated by silicon PN and NP junctions, enabling fast, polarity-switchable photoresponses. The negative photoconductivity, achieved without relying on defect states, supports sub-millisecond switching and on-chip differential signal processing. This platform holds strong potential for intelligent vision and AI-assisted optoelectronic systems.

Acknowledgment

The MoS_2 were characterized at the Instrumental Analytical Center, Shanghai Jiao Tong University.

References

[1] L. Mennel, J. Symonowicz, S. Wachter, D. K. Polyushkin, A. J. Molina-Mendoza, and T. Mueller, "Ultrafast machine vision with 2D material neural network image sensors," *Nature*, vol. 579, no. 7797, pp. 62–66, Mar. 2020, doi: 10.1038/s41586-020-2038-x.

[2] X. Han, J. Tao, Y. Liang, F. Guo, Z. Xu, W. Wu, J. Tong, M. Chen, C. Pan, and J. Hao, "Ultraweak light-modulated heterostructure with bidirectional photoresponse for static and dynamic image perception," *Nature Commun.*, vol. 15, no. 1, p. 10430, Nov. 2024, doi: 10.1038/s41467-024-54845-3.

[3] C.-Y. Wang, S.-J. Liang, S. Wang, P. Wang, Z. Li, Z. Wang, A. Gao, C. Pan, C. Liu, J. Liu, H. Yang, X. Liu, W. Song, C. Wang, B. Cheng, X. Wang, K. Chen, Z. Wang, K. Watanabe, T. Taniguchi, J. J. Yang, and F. Miao, "Gate-tunable van der Waals heterostructure for reconfigurable neural network vision sensor," *Sci. Adv.*, vol. 6, no. 26, p. 6173, Jun. 2020, doi: 10.1126/sciadv.aba6173.

[4] B. Wang, S. Zhong, P. Xu, and H. Zhang, "Recent development and advances in photodetectors based on two-dimensional topological insulators," *J. Mater. Chem. C*, vol. 8, no. 44, pp. 15526–15574, Nov. 2020, doi: 10.1039/d0tc03410j.

[5] A. Pelella, A. Kumar, K. Intonti, O. Durante, S. De Stefano, X. Han, Z. Li, Y. Guo, F. Giubileo, L. Camilli, M. Passacantando, A. Zak, and A. Di Bartolomeo, "WS_2 nanotube transistor for photodetection and optoelectronic memory applications," *Small*, vol. 20, no. 44, Nov. 2024, Art. no. 2403965, doi: 10.1002/smll.202403965.

[6] H. Jiang, H. Ji, Z. Ma, D. Yang, J. Ma, M. Zhang, X. Li, M. Wang, Y. Li, X. Chen, D. Wu, X. Li, C. Shan, and Z. Shi, "Simultaneous achieving negative photoconductivity response and volatile resistive switching in Cs_2CoCl_4 single crystals towards artificial optoelectronic synapse," *Light, Sci. Appl.*, vol. 13, no. 1, p. 316, Dec. 2024, doi: 10.1038/s41377-024-01642-8.

[7] M. Li, F.-S. Yang, Y.-C. Hsiao, C.-Y. Lin, H.-M. Wu, S.-H. Yang, H.-R. Li, C.-H. Lien, C.-H. Ho, H.-J. Liu, W. Li, Y.-F. Lin, and Y.-C. Lai, "Low-voltage operational, low-power consuming, and high sensitive tactile switch based on 2D layered InSe tribotronics," *Adv. Funct. Mater.*, vol. 29, no. 19, May 2019, Art. no. 1809119, doi: 10.1002/adfm.201809119.

[8] J. A. Alexander-Webber, C. K. Groschner, A. A. Sagade, G. Tainter, M. F. Gonzalez-Zalba, R. Di Pietro, J. Wong-Leung, H. H. Tan, C. Jagadish, S. Hofmann, and H. J. Joyce, "Engineering the photoresponse of InAs nanowires," *ACS Appl. Mater. Interfaces*, vol. 9, no. 50, pp. 43993–44000, Dec. 2017, doi: 10.1021/acsami.7b14415.

[9] W. Li, S. Zhou, X. Xia, Y. Wang, K. Yang, T. Hao, X. Zhang, Q. Yang, Z. Ni, J. Jiang, J. Si, F. Zhang, and Z. Zhang, "Ultrahigh and tunable negative photoresponse in organic-gated carbon nanotube film field-effect transistors," *Adv. Funct. Mater.*, vol. 33, no. 48, Nov. 2023, Art. no. 2305724, doi: 10.1002/adfm.202305724.

[10] B. Wang, L. Wang, Y. Zhang, M. Yang, D. Lin, N. Zhang, Z. Jiang, M. Liu, Z. Zhu, and H. Hu, "Mixed-dimensional MoS_2/Ge heterostructure junction field-effect transistors for logic operation and photodetection," *Adv. Funct. Mater.*, vol. 32, no. 10, Mar. 2022, Art. no. 2110181, doi: 10.1002/adfm.202110181.

[11] T. Jiang, Y. Huang, and X. Meng, "CdS core-Au/MXene-based photodetectors: Positive deep-UV photoresponse and negative UV–Vis-NIR photoresponse," *Appl. Surf. Sci.*, vol. 513, May 2020, Art. no. 145813, doi: 10.1016/j.apsusc.2020.145813.

[12] J.-Y. Wu, Y. T. Chun, S. Li, T. Zhang, J. Wang, P. K. Shrestha, and D. Chu, "Broadband MoS_2 field-effect phototransistors: Ultrasensitive visible-light photoresponse and negative infrared photoresponse," *Adv. Mater.*, vol. 30, no. 7, Feb. 2018, Art. no. 1705880, doi: 10.1002/adma.201705880.

[13] N. S. Vorobeva, S. Bagheri, A. Torres, and A. Sinitskii, "Negative photoresponse in $Ti_3C_2T_x$ MXene monolayers," *Nanophotonics*, vol. 11, no. 17, pp. 3953–3960, Aug. 2022, doi: 10.1515/nanoph-2022-0182.

[14] B. Li, D. Ji, A. K. Hamouda, and S. Luo, "MXene-derived TiO_2 nanosheets/rGO heterostructures for superior sodium-ion storage," *ChemPhysMater*, vol. 4, no. 1, pp. 48–55, Jan. 2025, doi: 10.1016/j.chphma.2024.05.001.

[15] T. Van Nguyen, M. Tekalgne, T. P. Nguyen, Q. Van Le, S. H. Ahn, and S. Y. Kim, "Electrocatalysts based on MoS_2 and WS_2 for hydrogen evolution reaction: An overview," *Battery Energy*, vol. 2, no. 3, May 2023, Art. no. 20220057, doi: 10.1002/bte2.20220057.

[16] W. He, D. Wu, L. Kong, P. Yu, and G. Yang, "Giant negative photoresponse in van der Waals Graphene/$AgBiP_2Se_6$/Graphene trilayer heterostructures," *Adv. Mater.*, vol. 36, no. 16, Apr. 2024, Art. no. 2312541, doi: 10.1002/adma.202312541.

[17] F. Zheng, Z. Chen, J. Li, R. Wu, B. Zhang, G. Nie, Z. Xie, and H. Zhang, "A highly sensitive CRISPR-empowered surface plasmon resonance sensor for diagnosis of inherited diseases with femtomolar-level real-time quantification," *Adv. Sci.*, vol. 9, no. 14, May 2022, Art. no. 2105231, doi: 10.1002/advs.202105231.

[18] C. Zha, X. Yan, X. Yuan, Y. Zhang, and X. Zhang, "An artificial optoelectronic synapse based on an InAs nanowire phototransistor with negative photoresponse," *Opt. Quantum Electron.*, vol. 53, no. 10, p. 587, Sep. 2021, doi: 10.1007/s11082-021-03217-y.

[19] Z. Chen, H. Huang, J. Deng, C. Meng, Y. Zhang, T. Fan, L. Wang, S. Sun, Y. Liu, H. Lin, S. Li, Y. Bai, L. Gao, J. Qu, D. Fan, X. Zhang, and H. Zhang, "Light-guided genetic scissors based on phosphorene quantum dot," *Laser Photon. Rev.*, vol. 18, no. 11, Nov. 2024, Art. no. 2400777, doi: 10.1002/lpor.202400777.

[20] I. Lee, M. Kang, S. Park, C. Park, H. Lee, S. Bae, H. Lim, S. Kim, W. Hong, and S.-Y. Choi, "Healing donor defect states in CVD-grown MoS_2 field-effect transistors using oxygen plasma with a channel-protecting barrier," *Small*, vol. 20, no. 2, Jan. 2024, Art. no. 2305143, doi: 10.1002/smll.202305143.

[21] S. B. Desai, S. R. Madhvapathy, M. Amani, D. Kiriya, M. Hettick, M. Tosun, Y. Zhou, M. Dubey, J. W. Ager, D. Chrzan, and A. Javey, "Gold-mediated exfoliation of ultralarge optoelectronically-perfect monolayers," *Adv. Mater.*, vol. 28, no. 21, pp. 4053–4058, Jun. 2016, doi: 10.1002/adma.201506171.

[22] Y. Sun, L. Jiang, Z. Wang, Z. Hou, L. Dai, Y. Wang, J. Zhao, Y.-H. Xie, L. Zhao, Z. Jiang, W. Ren, and G. Niu, "Multiwavelength high-detectivity MoS_2 photodetectors with Schottky contacts," *ACS Nano*, vol. 16, no. 12, pp. 20272–20280, Dec. 2022, doi: 10.1021/acsnano.2c06062.

[23] K. F. Mak, C. Lee, J. Hone, J. Shan, and T. F. Heinz, "Atomically ThinMoS_2: A new direct-gap semiconductor," *Phys. Rev. Lett.*, vol. 105, no. 13, Sep. 2010, Art. no. 136805, doi: 10.1103/physrevlett.105.136805.

[24] G. Eda, H. Yamaguchi, D. Voiry, T. Fujita, M. Chen, and M. Chhowalla, "Photoluminescence from chemically exfoliated MoS_2," *Nano Lett.*, vol. 11, no. 12, pp. 5111–5116, Dec. 2011, doi: 10.1021/nl201874w.

[25] W. Li, X. Gong, Z. Yu, L. Ma, W. Sun, S. Gao, Ç. Köroğlu, W. Wang, L. Liu, T. Li, H. Ning, D. Fan, Y. Xu, X. Tu, T. Xu, L. Sun, W. Wang, J. Lu, Z. Ni, J. Li, X. Duan, P. Wang, Y. Nie, H. Qiu, Y. Shi, E. Pop, J. Wang, and X. Wang, "Approaching the quantum limit in two-dimensional semiconductor contacts," *Nature*, vol. 613, no. 7943, pp. 274–279, Jan. 2023, doi: 10.1038/s41586-022-05431-4.

[26] P.-C. Shen, C. Su, Y. Lin, A.-S. Chou, C.-C. Cheng, J.-H. Park, M.-H. Chiu, A.-Y. Lu, H.-L. Tang, M. M. Tavakoli, G. Pitner, X. Ji, Z. Cai, N. Mao, J. Wang, V. Tung, J. Li, J. Bokor, A. Zettl, C.-I. Wu, T. Palacios, L.-J. Li, and J. Kong, "Ultralow contact resistance between semimetal and monolayer semiconductors," *Nature*, vol. 593, no. 7858, pp. 211–217, May 2021, doi: 10.1038/s41586-021-03472-9.

[27] S. S. Mousavi Khaleghi, J. Wei, Y. Liu, Y. Wang, Z. Fan, K. Li, J. Chen, R. Kudrawiec, R. Yang, K. B. Crozier, and Y. Dan, "MoS_2 phototransistors photogated with a P-N junction diode," *ACS Nano*, vol. 19, no. 12, pp. 12053–12062, Mar. 2025, doi: 10.1021/acsnano.4c17837.

[28] M. Ichimura, H. Tajiri, T. Ito, and E. Arai, "Temperature dependence of carrier recombination lifetime in Si wafers," *J. Electrochem. Soc.*, vol. 145, no. 9, pp. 3265–3271, Sep. 1998, doi: 10.1149/1.1838796.

[29] N. H. Protik, C. Li, M. Pruneda, D. Broido, and P. Ordejón, "The elphbolt ab initio solver for the coupled electron-phonon Boltzmann transport equations," *npj Comput. Mater.*, vol. 8, no. 1, p. 28, Feb. 2022, doi: 10.1038/s41524-022-00710-0.